Taylor & Francis
Taylor & Francis Group

Journal of Toxicology and Environmental Health, Part A
Current Issues

ISSN: 1528-7394 (Print) 1087-2620 (Online) Journal homepage: https://www.tandfonline.com/loi/uteh20

# Dual contribution of surface charge and protein-binding affinity to the cytotoxicity of polystyrene nanoparticles in nonphagocytic A549 cells and phagocytic THP-1 cells

Sung-Hyun Hwang, Frank Thielbeer, Jiyoung Jeong, Youngju Han, Sunay V. Chankeshwara, Mark Bradley & Wan-Seob Cho

**To cite this article:** Sung-Hyun Hwang, Frank Thielbeer, Jiyoung Jeong, Youngju Han, Sunay V. Chankeshwara, Mark Bradley & Wan-Seob Cho (2016) Dual contribution of surface charge and protein-binding affinity to the cytotoxicity of polystyrene nanoparticles in nonphagocytic A549 cells and phagocytic THP-1 cells, Journal of Toxicology and Environmental Health, Part A, 79:20, 925-937, DOI: 10.1080/15287394.2016.1207117

**To link to this article:** https://doi.org/10.1080/15287394.2016.1207117

JOURNAL OF TOXICOLOGY AND ENVIRONMENTAL HEALTH, PART A
2016, VOL. 79, NO. 20, 925–937
http://dx.doi.org/10.1080/15287394.2016.1207117

Taylor & Francis
Taylor & Francis Group

# Dual contribution of surface charge and protein-binding affinity to the cytotoxicity of polystyrene nanoparticles in nonphagocytic A549 cells and phagocytic THP-1 cells

Sung-Hyun Hwang[a], Frank Thielbeer[b], Jiyoung Jeong[a], Youngju Han[a], Sunay V. Chankeshwara[b], Mark Bradley[b], and Wan-Seob Cho[a]

[a]Lab of Toxicology, Department of Medicinal Biotechnology, College of Health Sciences, Dong-A University, Busan, Republic of Korea; [b]EastChem, School of Chemistry, University of Edinburgh, Edinburgh, United Kingdom

**ABSTRACT**

Knowledge that links the physicochemical properties of nanoparticles (NP) to their toxicity is key to evaluating and understanding mechanisms underlying toxicity and developing appropriate testing methods for NP; however, this is currently limited since only a small set of NP have been used, with typically poor control of their physical properties. In this study, eight types of polystyrene NP (PLNP) were synthesized with different functional groups, but all based on an identical core. In vitro cell-based assays were performed to determine the influence of changes in physicochemical properties, such as charge, hydrodynamic size, and protein binding potential, in relation to NP-mediated toxicity. The PLNP were incubated with nonphagocytic A549 cells or phagocytic differentiated THP-1 cells for 4 h with/without fetal bovine serum (FBS), followed by incubation for 20 h in FBS-supplemented medium with/without a washing step, to assess cell-type specificity and impact of protein corona formation. The effect of surface charge on cytotoxicity differed between A549 cells and THP-1 cells. In nonphagocytic A549 cells, the zeta potential of PLNP exhibited a negative correlation with cytotoxicity, partly due to the level of coronated protein that might affect cellular uptake. In phagocytic THP-1 cells, the zeta potential of PLNP showed a positive correlation with cytotoxicity but coronated protein levels displayed no marked association with cytotoxicity, owing to the professional uptake efficacy of phagocytic cells. The consistency of our data with THP-1 cells with the surface charge paradigm in nanotoxicology suggests that phagocytic cells are the predominant targets for lung inflammatory reactions induced by PLNP.

**ARTICLE HISTORY**
Received 21 June 2016
Accepted 25 June 2016

Evaluation of the structure–toxicity relationship is one of the challenges in nanotoxicology and is important for the safety-by-design approach of nanotechnology (Oberdorster et al., 2015). Such an understanding would facilitate prescreening of nanoparticles (NP)-mediated toxicity and enable the design of biologically benign/safe NP (Braakhuis et al., 2014; Kermanizadeh et al., 2016). The first step in the evaluation of a structure–toxicity relationship would be recognition of the structural parameters that give rise to toxicity (or nontoxicity) endpoints.

Structural parameters play a crucial role when in combination; however, each parameter on its own exerts a significant biological effect. The main structural parameters of NP that need to be examined include surface area, size, shape, dissolution, surface charge, and surface reactivity (Nel et al., 2009; Yu et al., 2013; Hartmann et al., 2015). In the lung inflammation model, the surface area of low-solubility NP is a better dose metric than mass or number, while intrinsic factors such as surface charge and surface reactivity are responsible for the slope of the dose-response curve (Donaldson et al., 2013). Although effects of size might overlap with those of surface area (in some cases), size by itself may affect lung inflammation as it influences deposition, cellular uptake, and clearance of NP in the lung (Bakand et al., 2012). Dissolution or biopersistence was also reported to influence the toxicity of soluble toxins, which

**CONTACT** Professor Wan-Seob Cho wcho@dau.ac.kr Lab of Toxicology, Department of Medicinal Biotechnology, College of Health Sciences, Dong-A University, 37 Nakdong-dero, 550 beon-gil, Saha-gu, Busan 604-714, Republic of Korea.
Supplemental data for this article can be accessed at the publisher 's website

may play a critical role in acute lung injury and immunogenicity (Cho et al., 2011, 2012a; Hartmann et al., 2015). The role of functional groups on the surface of NP has been recognized since zeta potential was reported to be critical for membranolytic potential and inflammogenic potential in an in vitro hemolysis model (Cho et al., 2014) and in an in vivo lung inflammation model (Kim et al., 2015), respectively. However, the effect of surface functional groups on in vitro cell-based assay are not well characterized due to a lack of understanding with regard to cell-type specificity and complications induced by interaction of NP with various biomolecules (Kroll et al., 2012; Sohaebuddin et al., 2010).

Recently Fytianos et al. (2015) reported that surface properties but not surface charge of gold NP (AuNP) modulated uptake and release of pro-inflammatory cytokines in monocyte-derived dendritic cells. However, Hirsch et al. (2013) demonstrated that positively charged NP displayed higher cellular uptake in vitro compared to negatively charged or neutral NP. This effect was attributed to the colloidal stability and aggregation state of NP rather than just surface charge (Hirsch et al., 2013). Cell types influence cellular internalization of NP. It is of interest that similar uptake of positively and negatively charged AuNP was observed in phagocytic RAW 264.7 cells but higher cellular uptake of positively charged AuNP than negatively charged AuNP was noted in nonphagocytic HepG2 cells (Liu et al., 2013). The influence of surface property is further complicated by cell death (Carneiro and Barbosa, 2016). Positively and negatively charged AuNP was reported to induce apoptosis while neutral AuNP produced necrosis in human keratinocyte cell line (HaCaT) (Schaeublin et al., 2011). However most of the studies were performed with a limited set of NP usually comprising three types of NP, such as positive, neutral, and negative. Thus, further studies were warranted to assess more broadly the role of surface property of NP on NP-mediated toxicity.

Identification of the individual physicochemical parameters relevant to the toxicity of NP is a challenge, as structural parameters in combination influence the toxic endpoint attributed to NP. Tuning the structural parameters from an identical NP core may resolve this limitation. Thus, in this study amine-modified polystyrene NP ($_{NH2}$PLNP) were synthesized and seven different functional groups conjugated to the $_{NH2}$PLNP to produce eight types of surface-modified PLNP with an identical core. The major differences explored between these finely designed NP were surface charge, hydrodynamic size, and protein binding affinity. To identify the physicochemical parameters of NP that influence their in vitro mediated toxicity and cell-type specificity, a nonphagocytic cell (human alveolar type 2-like A549 cell) and a phagocytic cell (human monocytic differentiated THP-1 cell) were used. The cells were treated with PLNP in the presence or absence of fetal bovine serum (FBS) and physicochemical properties inducing cytotoxicity or proinflammatory cytokine expression were evaluated.

## Methods

### Materials

FBS, L-glutamine, penicillin, streptomycin, Dulbecco's phosphate-buffered saline (DPBS), Du lbecco's modified Eagle's Medium (DMEM), and Roswell Park Memorial Institute 1640 (RPMI-1640) were purchased from Life Technologies (Gaith ersburg, MD). Ninety-six-well plates were obtained from Thermo Scientific (Hudson, NH). Phorbol myristate acetate (PMA) and bovine serum albumin (BSA) were purchased from Sigma-Aldrich (St. Louis, MO). A549 cells and THP-1 cells were obtained from the European Collection of Animal Cell Cultures (Salisbury, UK) and the American Type Culture Collection (Manassas, VA), respectively. The Duoset enzyme-linked immunosor bent assay (ELISA) kits for interleukin-1β (IL-1β), IL-8, macrophage inflammatory protein-1β (MIP-1β), and tumor necrosis factor-α (TNF-α) were purchased from R&D Systems (Minneapolis, MN). 2',7 '-Dichlorofluorescin diacetate (DCFH-DA) was obtained from Calbiochem (La Jolla, CA).

### Synthesis of PLNP

To evaluate the role of surface functionalization on cell-NP interface, PLNP with an identical core but different surface functional groups were synthesized according to the previously described method (Cho et al., 2014; Thielbeer

et al., 2011). At first, aminomethyl-functionalized PLNP was synthesized in an emulsifier-free emulsion polymerization using styrene, divinylbenzene, and *p*-vinylbenzylamine hydrochloride. The aminomethyl group of the particles was subsequently modified with seven types of functional groups (amine, guanidinium, acetyl, zwitterionic, hydroxyl, polyethylene glycol [PEG], carboxyl, and sulfonic acid) to yield the respective particles (synthesis details can be found in the Supplemental Data). Finally, eight different PLNP were synthesized: amine ($_{NH2}$PLNP), guanidinium ($_{GD}$PLNP), acetyl ($_{AC}$PLNP), zwitterionic ($_{ZI}$PLNP), hydroxyl ($_{OH}$PLNP), PEG ($_{PEG}$PLNP), carboxyl ($_{COOH}$PLNP), and sulfonic acid ($_{SO3H}$PLNP).

### Physicochemical Characterization of PLNP

The solid content of the PLNP was determined by drying the PLNP suspension under vacuum (<20 bar) at 40°C overnight. To measure the primary diameter and morphology of PLNP, 10 µl of 20 mg/ml PLNP suspension in distilled water (DW) was dried overnight onto carbon-coated stubs under vacuum (<20 mbar) at 40°C with the gold-sputter coating and particles were visualized with a Phillips XL30CP scanning electron microscope (Phillips XL30CP, Eindhoven, The Netherlands). The hydrodynamic size and zeta potential of the PLNP in DW were evaluated using a Malvern Zetasizer Nano-ZS (Malvern, Malvern Hills, UK). Endotoxin levels in PLNP suspension at the highest dose for in vitro study (100 µg/ml in DW) were measured using an endpoint chromogenic *Limulus* amebocyte lysate (LAL) assay (Cambrex, Walkersville, MD). The limit of detection (LOD) for this assay was 0.1–1 endotoxin units (EU)/ml.

### Cell-Free Reactive Oxygen Species (ROS) Assay

To assess the intrinsic capability of overall reactive oxygen species (ROS) generation, the DCFH-DA assay was used in a cell-free condition according to the previously described method (Rushton et al., 2010). The final concentrations of PLNP were 12.5, 25, 50, and 100 µg/ml and fluorescence intensity was quantified at 485/590 nm using a Synergy HT Multimode Microplate Reader (Bio-Tek Instruments, Winooski, VT). NiO NP (size: 5.3 ± 1.9 nm, zeta potential: +48.9 ± 0.6 mV) at 100 µg/ml was used as a positive control, which was confirmed in our previous study (Jeong et al., 2016). The potential for ROS generation by PLNP was expressed as micromolar $H_2O_2$ equivalents using a standard curve (0, 0.625, 1.25, 2.5, 5, and 10 µ*M* $H_2O_2$).

### Protein Binding Affinity Assay Using Bovine Serum Albumin

Bovine serum albumin (BSA) was selected for determination of potential for protein binding of PLNP because BSA is the most abundant serum protein and it is one of the major components of the protein corona when various NP were incubated with serum (Ramezani and Rafii-Tabar 2015; Saptarshi et al., 2013). To determine intrinsic binding affinity of PLNP with serum albumin protein, PLNP at 100 µg/ml in DPBS were incubated with 100 µg/ml BSA for 4 h at 37°C with continuous agitation. After 4 h of incubation, PLNP-free supernatants were collected following 3 rounds of centrifugation at 15,000 × g for 10 min. Then the bicinchoninic acid (BCA) assay (Thermo Fischer Scientific, Rockford, IL) was performed to measure total protein levels. The levels of coronated protein of PLNP were calculated from the total reduced protein levels after incubation with PLNP.

### Cell Culture

To elucidate the role of surface charge of NP to the cytotoxic potential and cell-type specificity in the inhalation setting, "nonphagocytic" A549 human lung adenocarcinoma cell line and "phagocytic" differentiated THP-1 human leukemia cell line were employed. Cells were cultured at 37°C with 5% $CO_2$. A549 cells were cultured in DMEM containing 5% FBS, 2 m*M* L-glutamine, 100 IU/ml penicillin, and 100 U/ml streptomycin, and THP-1 cells were cultured in RPMI-1640 containing 10% FBS, 2 m*M* L-glutamine, 100 IU/ml penicillin, and 100 U/ml streptomycin. A549 cells were seeded in 96-well plates at a density of $2 \times 10^5$ cells/ml in a complete medium (DMEM containing 5% FBS) and incubated overnight until 80% confluence. THP-1 cells were seeded in 96-well plates at a density of $1 \times 10^6$ cells/ml in a complete medium (RPMI-1640 containing 10% FBS) with 10 ng/ml PMA and incubated for 2 d

to differentiate into macrophages. Cells were then washed with prewarmed DPBS three times before treatment with PLNP.

### Preparation of PLNP and Experimental Settings for In Vitro Study

To examine the role of surface functionalization of PLNP and impact of protein corona formation on toxicity of PLNP, the PLNP were dispersed in complete medium (DMEM for A549 cells and RPMI-1640 for THP-1 cells) or in an FBS-free medium without any other dispersants. For in vitro study, there were four experimental groups with the nomenclature FNoW, NoFNoW, FW, and NoFW, to assess not only whether serum protein affects behavior of PLNP but also the impact of early-stage cellular uptake (Table 1). PLNP were prepared at concentrations of 25, 50, and 100 μg/ml based upon a concentration-range identification study (19, 38, 75, 150, and 300 μg/ml) and briefly sonicated in a water-bath sonicator (Saehan-Sonic, Seoul, Korea) for 5 min to dissociate possible agglomerates.

### Treatment of PLNP in FNoW or NoFNoW Settings

To determine the influence of protein corona at an early stage of cellular uptake, data from FNoW were compared to results from NoFNoW. For the FNoW group, PLNP in a complete medium at 25, 50, or 100 μg/ml were incubated with cells for 24 h. For the NoFNoW group, PLNP in an FBS-free medium at 25, 50, or 100 μg/ml were incubated with cells for 4 h. Then, FBS (5% for A549 cells and 10% for THP-1 cells) was added to culture medium and incubated for an additional 20 h. Cytotoxicity was measured by trypan blue exclusion assay since this assay minimizes interference by NP, as previously described (Lee et al., 2015). To determine levels of proinflammatory cytokines in the cell-free supernatant, PLNP-free supernatant was collected by 3 rounds of centrifugation at 15,000 × g for 10 min followed by centrifugation of cell supernatant for 5 min at 800 × g. Proinflammatory cytokines (IL-8 for A549 cells; IL-1β, MIP-1β, and TNF-α for THP-1 cells) were measured in a cell-free supernatant using a Duoset ELISA kit.

**Table 1.** Nomenclature for the Four Types of In Vitro Experimental Settings.

| Nomenclature | First incubation (4 h) | Washing step | Second incubation (additional 20 h) |
|---|---|---|---|
| FNoW | With FBS | No | With FBS |
| NoFNoW | Without FBS | No | With FBS |
| FW | With FBS | Yes | With FBS |
| NoFW | Without FBS | Yes | With FBS |

### Treatment of PLNP in FW or NoFW Settings

In order to compare the effect of protein corona, which might mitigate cellular uptake and toxicity, cells were treated with PLNP at concentrations of 25, 50, or 100 μg/ml for 4 h in an FBS-free medium or in a complete medium (5% FBS for A549 cells and 10% FBS for THP-1 cells); 4-h incubation in an FBS-free medium is not cytotoxic (Lesniak et al., 2012). Then cells were washed 3 times with prewarmed DPBS to exclude floating PLNP and incubated for an additional 20 h in a fresh complete medium. After incubation, cytotoxicity and proinflammatory cytokine expression were measured as already described.

### Statistical Analysis

Data were expressed as mean ± SEM unless stated otherwise, and graphs and statistical analysis were performed using the GraphPad Prism Software (Ver. 6; GraphPad Software Inc., La Jolla, CA). Each treatment group was compared by one-way analysis of variance (ANOVA) with post hoc Tukey's pairwise comparisons. The correlation between physicochemical properties of PLNP and toxicity endpoints from A549 cells or THP-1 cells was determined by the Pearson correlation test. Statistical significance was considered at $p < .05$.

## Results

### Physicochemical Properties of PLNP

Because the mass of all types of PLNP was based on that of $_{NH2}$PLNP, the particle number of all types of PLNP is theoretically the same. Scanning electron microscopy (SEM) demonstrated that all types of PLNP were spherical, with the size of each NP slightly different from the others, with sizes ranging from 200 to 320 nm (Figure S1 and Table 2). The $_{PEG}$PLNP was

**Table 2.** Physicochemical Properties of the Polystyrene Nanoparticles (PLNP).

| PLNPs | Primary size (nm) | Hydrodynamic size (nm) | Polydispersity index (PDI) | Zeta potential (mV) | Coronated albumin (μg/ml) |
|---|---|---|---|---|---|
| $_{NH2}$PLNP | 193.8 ± 18.5 | 217.7 ± 1.11 | 0.01 ± 0.00 | 23.5 ± 1.5 | 3.68 ± 1.12 |
| $_{GD}$PLNP | 217.9 ± 27.4 | 247.7 ± 2.12 | 0.09 ± 0.01 | 31.7 ± 0.4 | 6.12 ± 1.8 |
| $_{AC}$PLNP | 208.5 ± 9.1 | 746.2 ± 28.54 | 0.27 ± 0.01 | −8.1 ± 4.8 | 5.82 ± 0.59 |
| $_{ZI}$PLNP | 216.0 ± 25.1 | 786.2 ± 12.52 | 0.45 ± 0.04 | −5.3 ± 0.8 | 4.90 ± 1.5 |
| $_{OH}$PLNP | 224.2 ± 19.7 | 690.6 ± 23.75 | 0.42 ± 0.05 | −23.1 ± 1 | 1.84 ± 1.06 |
| $_{PEG}$PLNP | 319.8 ± 46.3 | 1205 ± 20.34 | 0.35 ± 0.02 | −4.4 ± 0.6 | 9.48 ± 0.91 |
| $_{COOH}$PLNP | 214.4 ± 16.9 | 480.6 ± 8.09 | 0.49 ± 0.03 | −24.9 ± 0.7 | 0.00 ± 1.66 |
| $_{SO3H}$PLNP | 220.1 ± 10.9 | 505.1 ± 40.55 | 0.49 ± 0.08 | −41.5 ± 1.3 | 4.90 ± 0.5 |

demonstrated to be approximately 100 nm larger than other PLNP due to swelling of the particles in water. The hydrodynamic size of PLNP displayed agglomerations: $_{NH2}$PLNP and $_{GD}$PLNP were the least agglomerated and $_{COOH}$PLNP and $_{SO3H}$PLNP were slightly agglomerated with sizes ranging from 480 to 505 nm, and the others were moderately agglomerated with sizes ranging from 690 to 1205 nm (Table 2). The zeta potential of each PLNP displayed a diverse distribution pattern ranging from −41 to +31 mV in DW with narrow peaks in each case (Table 2). All types of PLNP at 100 μg/ml in DW contained no endotoxin contamination. The levels of coronated albumin protein were variable by the types of PLNP, with the highest binding affinity in $_{PEG}$PLNP and the lowest binding affinity in $_{COOH}$PLNP (Table 2). Protein repellence was not observed due to attachment of a small molecular weight PEG (PEG3). Serum albumin binding affinity may be influenced by the surface area of PLNP, since $_{PEG}$PLNP were 320 nm in size while others were approximately 220 nm, resulting in a potential significant difference in total surface area of particles in solution.

### Cell-Free ROS Generation Assay

To evaluate the intrinsic property of ROS generation, a cell-free DCFH-DA assay was performed. Although PLNP except for $_{COOH}$PLNP and $_{PEG}$PLNP produced a significant increase, the potential for the ROS generation by these PLNP was less than that induced by the positive control (NiO NP) (Figure S2).

### Cytotoxicity of PLNP to A549 Cells

Cytotoxicity data in the FNoW group indicated that $_{COOH}$PLNP, $_{OH}$PLNP, $_{PEG}$PLNP, and $_{NH2}$PLNP induced a significant cytotoxic response, while the others failed to markedly alter cytotoxicity (Figure 1A). In the NoFNoW group, $_{SO3H}$PLNP, $_{COOH}$PLNP, $_{OH}$PLNP, $_{ZI}$PLNP, and $_{PEG}$PLNP produced significant cytotoxicity compared to the vehicle control (Figure 1B). All types of PLNP in the FW group displayed no cytotoxicity, while only $_{OH}$PLNP induced a significant cytotoxic response (Figures 1C and 1D).

### IL-8 Expression by PLNP Treatment in A549 Cells

In the FNoW group, all PLNP significantly elevated IL-8 levels compared to the control (Figure 2A). The IL-8 expression pattern in NoFNoW group was similar to that of the FNoW group except for the $_{OH}$PLNP and $_{AC}$PLNP, which displayed no significant change (Figure 2B). In the FW group, PLNP did not significantly change IL-8 expression (Figure 2C). In the NoFW group, $_{SO3H}$PLNP, $_{AC}$PLNP, and $_{PEG}$PLNP displayed a significant rise in IL-8 expression (Figure 2D).

### Cytotoxicity of PLNP in Differentiated THP-1 Cells

In the FNoW group, treatment with $_{COOH}$PLNP, $_{OH}$PLNP, $_{AC}$PLNP, $_{ZI}$PLNP, and $_{NH2}$PLNP induced significant cytotoxicity in a concentration-dependent manner (Figure 3A). All PLNP in the NoFNoW group induced significant twofold higher cytotoxicity than FNoW (Figure 3B). When PLNP were incubated in the FW setting, no marked change was observed. In contrast, all PLNP in the NoFW setting except for $_{ZI}$PLNP were significantly cytotoxic (Figures 3C and 3D).

### IL-1β Expression by PLNP Treatment in Differentiated THP-1 Cells

In the FNoW group, IL-1β expression was significantly increased following $_{COOH}$PLNP, $_{OH}$PLNP, $_{AC}$PLNP, and $_{PEG}$PLNP treatment compared to

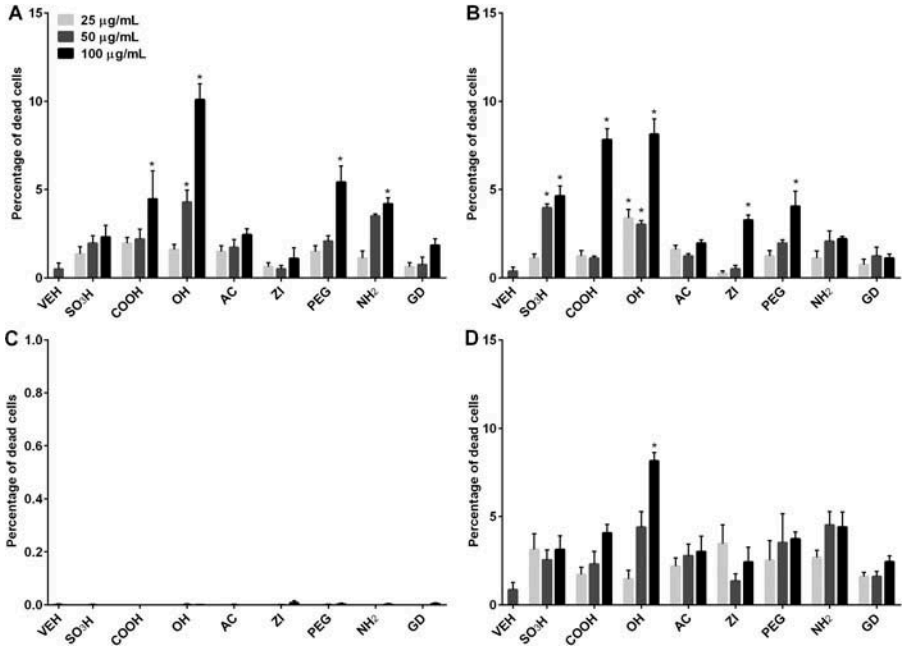


**Figure 1.** Cytotoxicity evaluation of PLNP with A549 cells by the trypan blue exclusion assay. PLNP were prepared at concentrations of 25, 50, or 100 μg/ml under the following experimental settings: (A) FNoW; (B) NoFNoW; (C) FW; (D) NoFW. Data are expressed as mean ± SEM and $n = 4$; asterisk indicates significant at $p < .05$ relative to vehicle control (VEH).

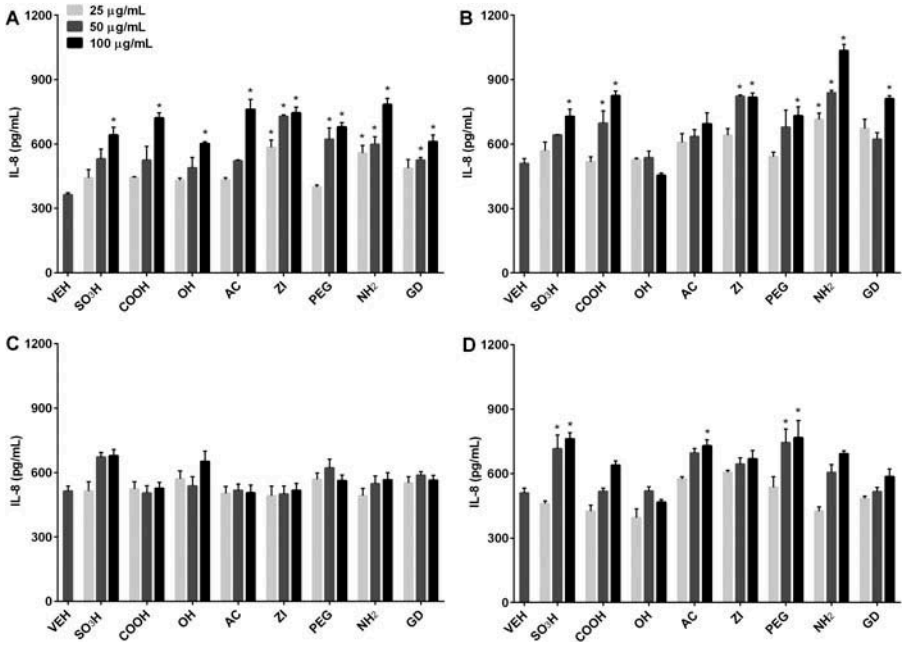


**Figure 2.** Expression of IL-8 of A549 cells after exposure to eight types of PLNP. PLNP were prepared at concentrations of 25, 50, or 100 μg/ml under the following experimental settings: (A) FNoW; (B) NoFNoW; (C) FW; (D) NoFW. Data are expressed as mean ± SEM and $n = 4$; asterisk indicates significant at $p < .05$ relative to vehicle control (VEH).

the control (Figure 4A). The NoFNoW group generally displayed approximately 10-fold higher levels of IL-1β than FNoW, but the pattern was similar to that of FNoW except for $_{SO3H}$PLNP and $_{NH2}$PLNP, which demonstrated a marked rise in the NoFNoW setting (Figure 4B). In the FW group, only $_{OH}$PLNP and $_{PEG}$PLNP significantly elevated IL-1β expression (Figure 4C). In the NoFW group, $_{COOH}$PLNP, $_{OH}$PLNP, and $_{NH2}$PLNP significantly increased IL-1β expression compared to the control (Figure 4D).

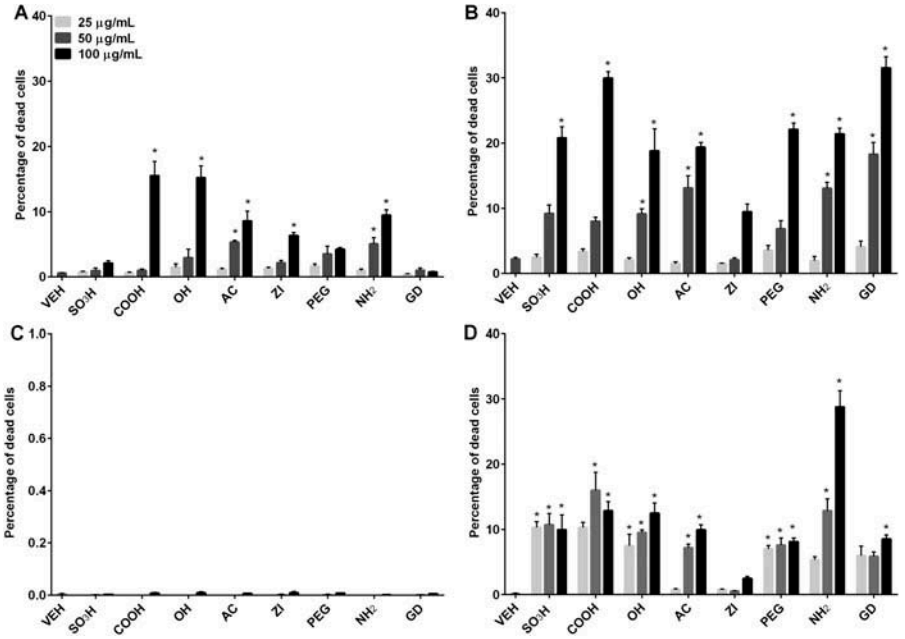


**Figure 3.** Cytotoxicity assessment of PLNP with THP-1 cells by trypan blue exclusion assay. THP-1 cells were differentiated for 2 d, followed by treatment with PMA (10 ng/ml) and PLNP at 25, 50, or 100 μg/ml prepared under the following experimental settings: (A) FNoW; (B) NoFNoW; (C) FW; (D) NoFW. Data are expressed as mean ± SEM and $n = 4$; asterisk indicates significant at $p < .05$ relative to vehicle control (VEH).

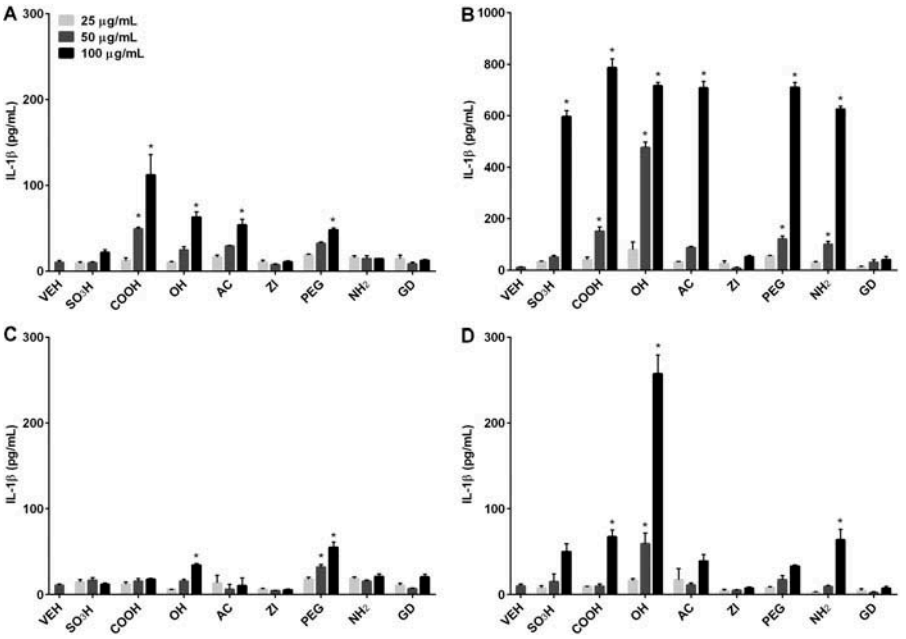


**Figure 4.** IL-1β expression in differentiated THP-1 cells after exposure to eight types of PLNP. THP-1 cells were differentiated for 2 d, followed by treatment with PMA (10 ng/ml) and PLNP at 25, 50, or 100 μg/ml prepared under the following experimental settings: (A) FNoW; (B) NoFNoW; (C) FW; (D) NoFW. Data are expressed as mean ± SEM and $n = 4$; asterisk indicates significant at $p < .05$ relative to vehicle control (VEH).

### MIP-1β Expression by PLNP Treatment in Differentiated THP-1 Cells

The MIP-1β expression in the FNoW group was significantly elevated by $_{COOH}$PLNP, $_{OH}$PLNP, $_{AC}$PLNP, and $_{PEG}$PLNP. However, in the NoFNoW group, all types of PLNP significantly increased MIP-1β expression (Figures 5A and 5B). In the FW group, only $_{PEG}$PLNP treatment produced a significant rise; however, the increase was less than for other experimental settings (Figure 5C). All types of PLNP except for $_{ZI}$PLNP and $_{GD}$PLNP significantly enhanced expression of MIP-1β in the NoFW setting with similar magnitude compared to FNoW or NoFNoW (Figure 5D).

### TNF-α Expression by PLNP Treatment in Differentiated THP-1 Cells

In the FNoW group, $_{COOH}$PLNP, $_{AC}$PLNP, and $_{PEG}$PLNP showed a significant increase in TNF-α expression compared to the control (Figure 6A). Elevated TNF-α expression was noted in the NoFNoW group to a greater extent than for other settings and all types of PLNP except for $_{ZI}$PLNP and $_{GD}$PLNP (Figure 6B). In the FW group, none of the treatments produced a significant alteration in TNF-α levels (Figure 6C). In the NoFW group, only $_{OH}$PLNP significantly increased TNF-α levels (Figure 6D).

### Correlation Between Physiochemical Property of PLNPs and Toxicity Endpoints of A549 Cells

The zeta potential of PLNP displayed a significant negative correlation with the cytotoxicity of PLNP in the NoFNoW group (Figure 7). The levels of coronated protein of PLNP showed no marked correlation with cytotoxicity. However, the negative trend between the two parameters was evident with the exclusion of the PEG group, which possessed increased hydrodynamic size and consequent significant correlation. The hydrodynamic size displayed no significant pattern (Figure S3). All plots between physicochemical property and cytotoxicity in FNoW and NoFW exhibited no significant trend (Figure S3). In addition, the levels of IL-8 expression demonstrated no specific relationship with tested physicochemical properties (data not shown).

### Correlation Between Physiochemical Property of PLNP and Toxicity Endpoints of Differentiated THP-1 Cells

The zeta potential of PLNP displayed a positive trend with cytotoxicity of THP-1 cells in both the FNoW and NoFNoW groups (Figure 8). However, the positive trend was only significant when $_{GD}$PLNP in the FNoW group and $_{ZI}$PLNP in the NoFNoW group were excluded. $_{GD}$PLNP was

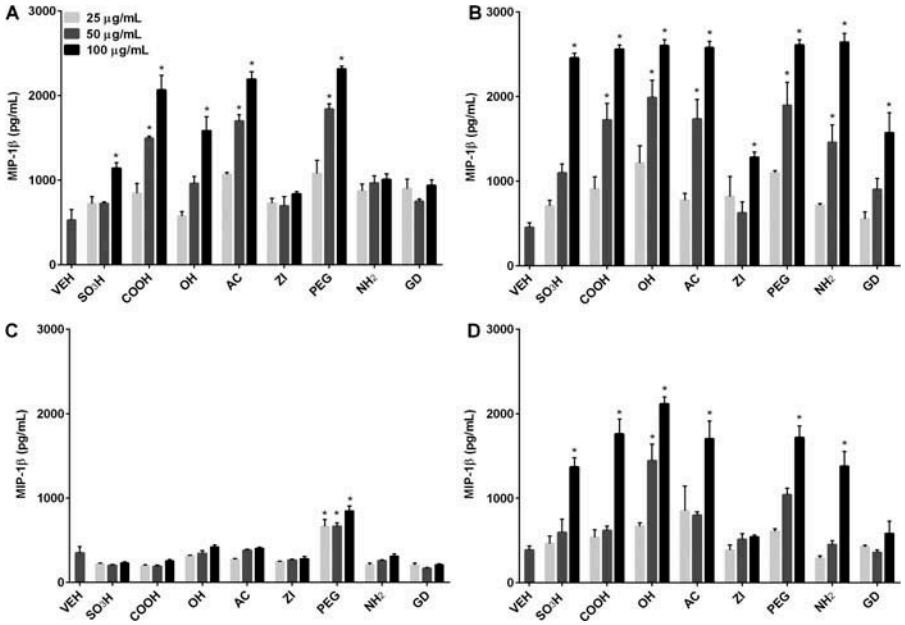


**Figure 5.** MIP-1β expression in differentiated THP-1 cells after exposure to eight types of PLNP. THP-1 cells were differentiated for 2 d, followed by treatment with PMA (10 ng/ml) and PLNP at 25, 50, or 100 μg/ml with the following experimental settings: (A) FNoW; (B) NoFNoW; (C) FW; (D) NoFW. Data are expressed as mean ± SEM and $n = 4$; asterisk indicates significant at $p < .05$ relative to vehicle control (VEH).

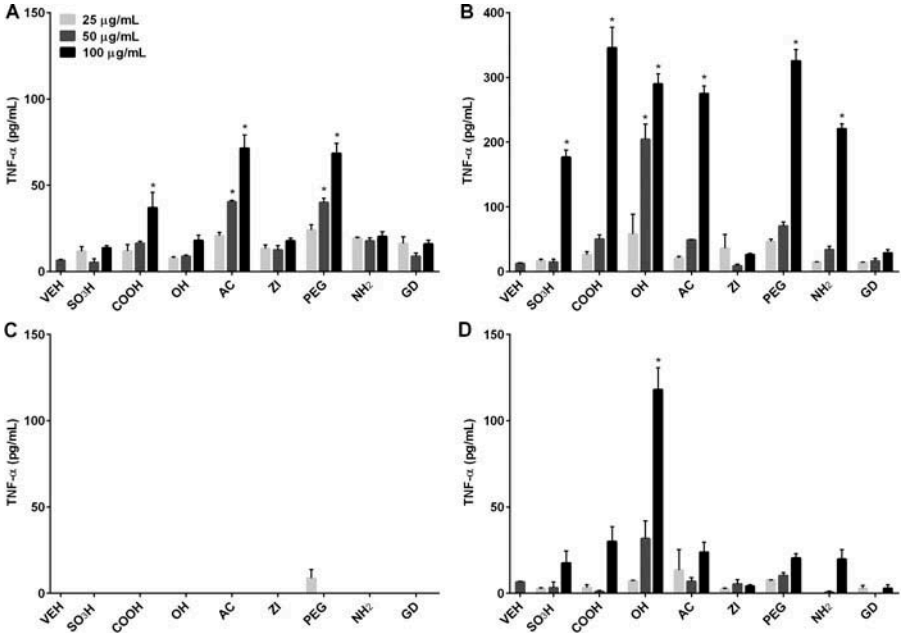


**Figure 6.** TNF-α expression in differentiated THP-1 cells after exposure to eight types of PLNP. THP-1 cells were differentiated for 2 d, followed by treatment with PMA (10 ng/ml) and PLNP at 25, 50, or 100 μg/ml prepared under the following experimental settings: (A) FNoW; (B) NoFNoW; (C) FW; (D) NoFW. Data are expressed as mean ± SEM and $n = 4$; asterisk indicates significant at $p < .05$ relative to vehicle control (VEH).

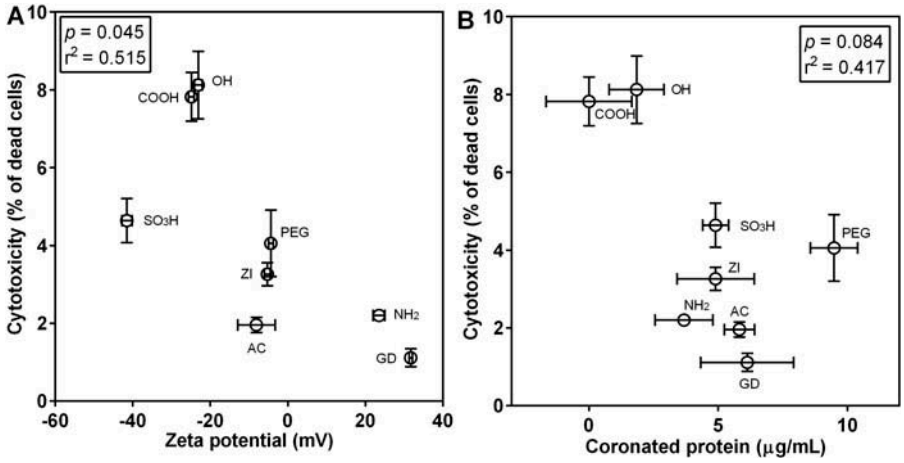


**Figure 7.** Correlation between physicochemical properties and cytotoxicity of PLNP at high concentration (100 μg/ml) in non-phagocytic A549 cells. (A) Cytotoxicity data were plotted against the zeta potential in the NoFNoW group. (B) Cytotoxicity results were plotted against coronated albumin protein levels in the NoFNoW group. The $p$ and $r^2$ values in the inset were obtained by the Pearson correlation test. Full-scale analysis is presented in Figure S3.

excluded in this correlation since it was markedly affected by serum albumin protein. $_{GD}$PLNP decreased cytotoxicity in the FNoW group but elevated cytotoxicity in the NoFNoW group. The levels of coronated protein exhibited no trend for cytotoxicity in both the FNoW and NoFNoW groups (Figure S4). However, in the NoFW group, levels of coronated protein demonstrated a negative trend with cytotoxicity, and exclusion of the $_{ZI}$PLNP group produced a significant response. In all experimental settings, hydrodynamic size displayed no marked relationship with NP cytotoxicity. Similarly, the proinflammatory cytokine expression was found not correlated with any physicochemical properties (data not shown).

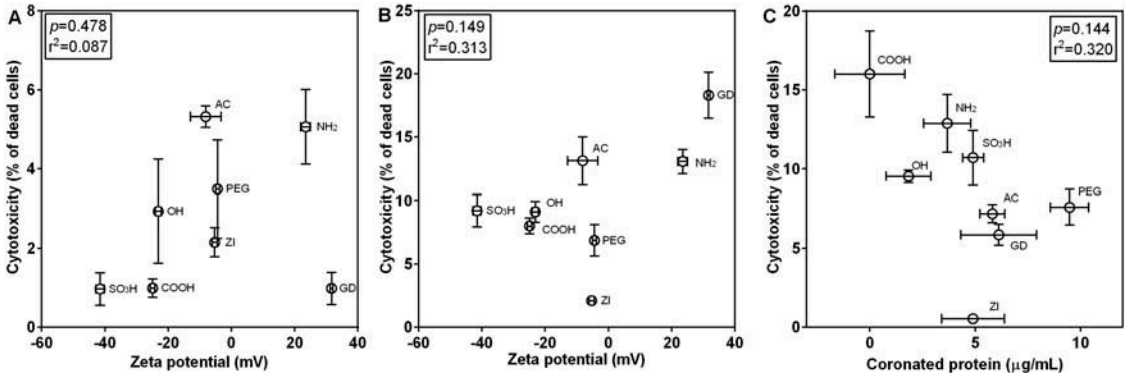


**Figure 8.** Correlation between physicochemical properties and cytotoxicity of PLNP at mid-concentration (50 μg/ml) in phagocytic THP-1 cells. Cytotoxicity data in FNoW (A) or NoFNoW (B) are plotted against the zeta potential of PLNP. (C) Cytotoxicity results in the NoFW group are plotted against coronated protein levels. The $p$ and $r^2$ values in the inset were obtained by the Pearson correlation test. Full-scale analysis is presented in Figure S4.

## Discussion

Cell-based assays are performed to ensure consistency with in vivo assays and are used for evaluation of mechanisms observed in phenomenological animal bioassays. Unfortunately, most in vitro toxicity studies with NP are not consistent with in vivo bioassays owing to various factors including dosimetry, cell-type specificity, dynamic changes of physicochemical properties, and interference in assays (Guadagnini et al., 2015; Oberdorster et al., 2015; Sohaebuddin et al., 2010). Nevertheless, the development of a gold-standard in vitro assay is inevitable owing to the 3R (Replacement, Reduction, and Refinement) policy in animal bioassays and the need for rapid and high-throughput screening assays (Cho et al., 2013). Understanding the effect of physicochemical properties of NP on toxicity marks the first step for in vitro assays. The role of surface functionalization of NP on NP-mediated toxicity toward nonphagocytic A549 cells or phagocytic differentiated THP-1 cells using eight types of PLNP was thus examined.

In this study, the NoFNoW group produced increased cytotoxicity and proinflammatory cytokine expression in both cell lines, compared to FNoW. These two groups differed only in the early-stage (4 h) incubation where one group was exposed without serum protein; however, the incubation condition in the late stage (20 h) remained the same. Comparison of the NoFW and FW groups also indicated the importance of the early stage of incubation, which warrants further investigation to identify a better system that simulates in vivo conditions. The enhanced toxicity in the serum-deprived condition compared to the serum-supplemented one was more prominent in phagocytic differentiated THP-1 cells than in nonphagocytic A549 cells since the biologically effective concentration for NP is correlated with the total amount NP within cells (Donaldson et al., 2013; Liu et al., 2013) and protein corona reducing uptake (phagocytosis in most cases) of NP (Lesniak et al., 2012).

In this study, a trend was identified between the zeta potential of PLNP and in vitro toxicity endpoints. Exposure to NoFNoW for A549 cells, zeta potential for all PLNP, and levels of the coronated protein excluding $_{PEG}$PLNP showed a significant negative trend with cytotoxicity. Positively charged NP were generally reported to have higher uptake efficacy than negatively charged counterparts (Frohlich, 2012). In contrast, carboxylated PLNP displayed higher uptake by alveolar type I cells than aminated PLNP (Kemp et al., 2008). The discrepancy among these studies might be attributed to the limited set of NP, which are not sufficient to affirm the surface charge paradigm (Lorenz et al., 2006). Further, physicochemical properties such as protein binding affinity may also contribute to the observed differences. The negative correlation between zeta potential and cytotoxicity in nonphagocytic A549 cells might be associated with protein-binding affinity since positively charged PLNP displayed higher binding affinity than negatively charged ones. The serum

protein corona in turn reduced cellular uptake especially in nonphagocytic A549 cells (Lesniak et al., 2013). The effect of hydrodynamic size in this study showed no specific correlation with toxicity endpoints since hydrodynamic size of each type of PLNP was more than 200 nm, which exceeds the size range for the highest uptake (20–50 nm) in nonphagocytic cells (Chithrani et al., 2006; Jiang et al., 2008).

In contrast to the zeta potential of PLNP in nonphagocytic A549 cells, the zeta potential of PLNP except $_{GD}$PLNP or $_{ZI}$PLNP exhibited a positive trend with cytotoxicity in phagocytic THP-1 cells. $_{GD}$PLNP and $_{ZI}$PLNP were excluded from this correlation, since protein binding was important for these PLNP, which warrants further studies. Evidence indicates that various physicochemical properties and their combinations need to be considered while evaluating toxicity of NP. The levels of coronated protein of PLNP demonstrated a negative trend with respect to cytotoxicity of THP-1 cells at the early stage of exposure (4 h), but no marked effect was observed at a later stage of exposure (20 h). These findings are consistent with those of Liu et al. (2013), who reported that enhanced phagocytic activity of RAW 264.7 cells aids uptake of both negatively and positively charged Au NP to a similar extent. These results also indicated that protein corona exerted little influence on cellular uptake in phagocytic THP-1 cells, in contrast to nonphagocytic A549 cells. Therefore, positively charged PLNP display increased cytotoxicity in THP-1 cells compared to negatively charged ones even though each type of PLNP was engulfed to a similar extent. The electrostatic attractive force between positively charged PLNP and negatively charged lysosomal membrane might produce resultant toxicity (Cho et al., 2012b; Panyam et al., 2002).

A major observation in this study is the correlation between zeta potential and cytotoxicity of phagocytic differentiated THP-1 cells, which was consistent with in vivo lung inflammation studies (Cho et al., 2012b; Kim et al., 2015; Li et al., 2013). Data suggest that phagocytic cells are the predominant target cells for acute lung inflammation induced by PLNP, and that phagocytic cells may be employed to evaluate the mechanism underlying inflammogenicity of NP. Findings of proinflammatory cytokines from both cell lines indicate that proinflammatory cytokines have limited utility as toxicity endpoints; however, these measurements of these components may serve a role in evaluation of the mechanism of toxicity.

## Conclusions

The role of surface functionalization in the toxicity of NP was examined using eight types of custom-designed PLNP. The influence of surface charge on NP cytotoxicity differed between nonphagocytic A549 cells and phagocytic THP-1 cells as follows:

- In nonphagocytic A549 cells, the zeta potential of PLNP showed a negative trend with respect to cytotoxicity, which was partly attributed to coronated protein levels that reduce cellular uptake.
- In phagocytic THP-1 cells, the zeta potential of PLNP demonstrated a positive trend with respect to cytotoxicity in phagocytic THP-1 cells even though the coronated protein levels showed no marked correlation, which was attributed to increased cellular uptake efficacy of phagocytic cells.
- The consistency between our data from THP-1 cells and previous in vivo studies indicates that phagocytic cells are the predominant targets for lung inflammation induced by NP.

## Funding

This study was supported by grants from the Dong-A University.

## Declaration of Interest

The authors report no conflicts of interest. The authors alone are responsible for the content and writing of the article.

## References

Bakand, S., Hayes, A., and Dechsakulthorn, F. 2012. Nanoparticles: A review of particle toxicology following inhalation exposure. *Inhal. Toxicol.* 24: 125–135.

Braakhuis, H. M., Park, M. V., Gosens, I., De Jong, W. H., and Cassee, F. R. 2014. Physicochemical characteristics of nanomaterials that affect pulmonary inflammation. *Part. Fibre Toxicol.* 11: 18.

Carneiro, M. F. H., and Barbosa, F., Jr. 2016. Gold nanoparticles: A critical review of therapeutic applications and toxicological aspects. *J. Toxicol. Environ. Health B* 19: 129–148.

Chithrani, B. D., Ghazani, A. A., and Chan, W. C. 2006. Determining the size and shape dependence of gold nanoparticle uptake into mammalian cells. *Nano Lett*. 6: 662–668.

Cho, W. S., Duffin, R., Bradley, M., Megson, I. L., MacNee, W., Howie, S. E. M., and Donaldson, K. 2012a. NiO and $Co_3O_4$ nanoparticles induce lung DTH-like responses and alveolar lipoproteinosis. *Eur. Respir. J*. 39: 546–557.

Cho, W. S., Duffin, R., Bradley, M., Megson, I. L., Macnee, W., Lee, J. K., Jeong, J., and Donaldson, K. 2013. Predictive value of in vitro assays depends on the mechanism of toxicity of metal oxide nanoparticles. *Part. Fibre Toxicol*. 10: 55.

Cho, W. S., Duffin, R., Howie, S. E., Scotton, C. J., Wallace, W. A., Macnee, W., Bradley, M., Megson, I. L., and Donaldson, K. 2011. Progressive severe lung injury by zinc oxide nanoparticles: The role of $Zn^{2+}$ dissolution inside lysosomes. *Part. Fibre Toxicol*. 8: 27.

Cho, W. S., Duffin, R., Thielbeer, F., Bradley, M., Megson, I. L., Macnee, W., Poland, C. A., Tran, C. L., and Donaldson, K. 2012b. Zeta potential and solubility to toxic ions as mechanisms of lung inflammation caused by metal/metal oxide nanoparticles. *Toxicol. Sci*. 126: 469–477.

Cho, W. S., Thielbeer, F., Duffin, R., Johansson, E. M., Megson, I. L., Macnee, W., Bradley, M., and Donaldson, K. 2014. Surface functionalization affects the zeta potential, coronal stability and membranolytic activity of polymeric nanoparticles. *Nanotoxicology* 8: 202–211.

Donaldson, K., Schinwald, A., Murphy, F., Cho, W. S., Duffin, R., Tran, L., and Poland, C. 2013. The biologically effective dose in inhalation nanotoxicology. *Acc. Chem. Res*. 46: 723–732.

Frohlich, E. 2012. The role of surface charge in cellular uptake and cytotoxicity of medical nanoparticles. *Int. J. Nanomed*. 7: 5577–5591.

Fytianos, K., Rodriguez-Lorenzo, L., Clift, M. J., Blank, F., Vanhecke, D., von Garnier, C., Petri-Fink, A., and Rothen-Rutishauser, B. 2015. Uptake efficiency of surface modified gold nanoparticles does not correlate with functional changes and cytokine secretion in human dendritic cells in vitro. *Nanomed. Nanotechnol. Biol. Med*. 11: 633–644.

Guadagnini, R., Halamoda Kenzaoui, B., Walker, L., Pojana, G., Magdolenova, Z., Bilanicova, D., Saunders, M., Juillerat-Jeanneret, L., Marcomini, A., Huk, A., Dusinska, M., Fjellsbo, L. M., Marano, F., and Boland, S. 2015. Toxicity screenings of nanomaterials: Challenges due to interference with assay processes and components of classic in vitro tests. *Nanotoxicology* 9: 13–24.

Hartmann, N. B., Jensen, K. A., Baun, A., Rasmussen, K., Rauscher, H., Tantra, R., Cupi, D., Gilliland, D., Pianella, F., and Riego Sintes, J. M. 2015. Techniques and protocols for dispersing nanoparticle powders in aqueous media—Is there a rationale for harmonization? *J. Toxicol. Environ. Health B* 18: 299–326.

Hirsch, V., Kinnear, C., Moniatte, M., Rothen-Rutishauser, B., Clift, M. J., and Fink, A. 2013. Surface charge of polymer coated SPIONs influences the serum protein adsorption, colloidal stability and subsequent cell interaction in vitro. *Nanoscale* 5: 3723–3732.

Jeong, J., Kim, J., Seok, S. H., and Cho, W. S. 2016. Indium oxide ($In_2O_3$) nanoparticles induce progressive lung injury distinct from lung injuries by copper oxide (CuO) and nickel oxide (NiO) nanoparticles. *Arch. Toxicol*. 90: 817–828.

Jiang, W., Kim, B. Y., Rutka, J. T., and Chan, W. C. 2008. Nanoparticle-mediated cellular response is size-dependent. *Nat. Nanotechnol*. 3: 145–150.

Kemp, S. J., Thorley, A. J., Gorelik, J., Seckl, M. J., O'Hare, M. J., Arcaro, A., Korchev, Y., Goldstraw, P., and Tetley, T. D. 2008. Immortalization of human alveolar epithelial cells to investigate nanoparticle uptake. *Am. J. Respir. Cell Mol. Biol*. 39: 591–597.

Kermanizadeh, A., Gosens, I., MacCalman, L., Johnston, H., Danielsen, P. H., Jacobsen, N. R., Lenz, A. G., Fernades, T., Schins, R. P., Cassee, F. R., Wallin, H., Kryeling, W., Stoeger, T., Loft, S., Møller, P., Tran, L., and Stone, V. 2016. A multilaboratory toxicological assessment of a panel of 10 engineered nanomaterials to human health–ENPRA Project—The highlights, limitations, and current and future challenges. *J. Toxicol. Environ. Health B* 19: 1–28.

Kim, J., Chankeshwara, S. V., Thielbeer, F., Jeong, J., Donaldson, K., Bradley, M., and Cho, W. S. 2015. Surface charge determines the lung inflammogenicity: A study with polystyrene nanoparticles. *Nanotoxicology* 6: 1–8.

Kroll, A., Pillukat, M. H., Hahn, D., and Schnekenburger, J. 2012. Interference of engineered nanoparticles with in vitro toxicity assays. *Arch. Toxicol*. 86: 1123–1136.

Lee, Y. G., Jeong, J., Raftis, J., and Cho, W. S. 2015. Determination of adsorption affinity of nanoparticles for interleukin-8 secreted from A549 cells by in vitro cell-free and cell-based assays. *J. Toxicol. Environ. Health A* 78: 185–195.

Lesniak, A., Fenaroli, F., Monopoli, M. P., Aberg, C., Dawson, K. A., and Salvati, A. 2012. Effects of the presence or absence of a protein corona on silica nanoparticle uptake and impact on cells. *ACS Nano* 6: 5845–5857.

Lesniak, A., Salvati, A., Santos-Martinez, M. J., Radomski, M. W., Dawson, K. A., and Aberg, C. 2013. Nanoparticle adhesion to the cell membrane and its effect on nanoparticle uptake efficiency. *J. Am. Chem. Soc*. 135: 1438–1444.

Li, R., Wang, X., Ji, Z., Sun, B., Zhang, H., Chang, C. H., Lin, S., Meng, H., Liao, Y. P., Wang, M., Li, Z., Hwang, A. A., Song, T. B., Xu, R., Yang, Y., Zink, J. I., Nel, A. E., and Xia, T. 2013. Surface charge and cellular processing of covalently functionalized multiwall carbon nanotubes determine pulmonary toxicity. *ACS Nano* 7: 2352–2368.

Liu, X., Huang, N., Li, H., Jin, Q., and Ji, J. 2013. Surface and size effects on cell interaction of gold nanoparticles with both phagocytic and non-phagocytic cells. *Langmuir* 29: 9138–9148.

Lorenz, M. R., Holzapfel, V., Musyanovych, A., Nothelfer, K., Walther, P., Frank, H., Landfester, K., Schrezenmeier, H., and Mailander, V. 2006. Uptake of functionalized, fluorescent-labeled polymeric particles

in different cell lines and stem cells. *Biomaterials* 27: 2820–2828.

Nel, A. E., Madler, L., Velegol, D., Xia, T., Hoek, E. M., Somasundaran, P., Klaessig, F., Castranova, V., and Thompson, M. 2009. Understanding biophysicochemical interactions at the nano–bio interface. *Nat. Mater.* 8: 543–557.

Oberdorster, G., Castranova, V., Asgharian, B., and Sayre, P. 2015. Inhalation exposure to carbon nanotubes (CNT) and carbon nanofibers (CNF): Methodology and dosimetry. *J. Toxicol. Environ. Health B* 18:121–212.

Panyam, J., Zhou, W. Z., Prabha, S., Sahoo, S. K., and Labhasetwar, V. 2002. Rapid endo-lysosomal escape of poly(DL-lactide-co-glycolide) nanoparticles: Implications for drug and gene delivery. *FASEB J.* 16: 1217–1226.

Ramezani, F., and Rafii-Tabar, H. 2015. An in-depth view of human serum albumin corona on gold nanoparticles. *Mol. Biosyst.* 11: 454–462.

Rushton, E. K., Jiang, J., Leonard, S. S., Eberly, S., Castranova, V., Biswas, P., Elder, A., Han, X., Gelein, R., Finkelstein, J., and Oberdorster, G. 2010. Concept of assessing nanoparticle hazards considering nanoparticle dosemetric and chemical/biological response metrics. *J. Toxicol. Environ. Health A* 73: 445461.

Saptarshi, S. R., Duschl, A., and Lopata, A. L. 2013. Interaction of nanoparticles with proteins: Relation to bio-reactivity of the nanoparticle. *J. Nanobiotechnol.* 11: 26.

Schaeublin, N. M., Braydich-Stolle, L. K., Schrand, A. M., Miller, J. M., Hutchison, J., Schlager, J. J., and Hussain, S. M. 2011. Surface charge of gold nanoparticles mediates mechanism of toxicity. *Nanoscale* 3: 410–420.

Sohaebuddin, S. K., Thevenot, P. T., Baker, D., Eaton, J. W., and Tang, L. 2010. Nanomaterial cytotoxicity is composition, size, and cell type dependent. *Part. Fibre Toxicol.* 7: 22.

Thielbeer, F., Donaldson, K., and Bradley, M. 2011. Zeta potential mediated reaction monitoring on nano and microparticles. *Bioconj. Chem.* 22: 144–150.

Yu, K. N., Kim, J. E., Seo, H. W., Chae, C., and Cho, M. H. 2013. Differential toxic responses between pristine and functionalized multiwall nanotubes involve induction of autophagy accumulation in murine lung. *J. Toxicol. Environ. Health A* 76:1282–1292.